Chinese Chemical Letters 33 (2022) 5120–5123

Contents lists available at ScienceDirect

Chinese Chemical Letters

journal homepage: www.elsevier.com/locate/cclet

A multiple-function fluorescent pillar[5]arene: Fe^{3+}/Ag^{+} detection and light-harvesting system

Yang Luo, Wei Zhang, Qian Ren, Guo-Rong Chen, Jiang-Lian Ran, Xin Xiao*

Key Laboratory of Macrocyclic and Supramolecular Chemistry of Guizhou Province, Guizhou University, Guiyang 550025, China

ARTICLE INFO

Article history:
Received 8 February 2022
Revised 9 April 2022
Accepted 12 April 2022
Available online 15 April 2022

Keywords:
Pillar[5]arene
Modification
Energy transfer system
Metal detection

ABSTRACT

A novel pillar[5]arene (P5DPB) that includes a classical π-conjugated molecule, 4,4′-(1,4-phenylenedi-2,1-ethenediyl) bis-pyridine (DPB), was designed and synthesized as a substituent. Because of this modification, P5DPB exhibits several unique properties that differ from those of common pillar[5]arenes. The P5DPB neutral pyridine shows good selectivity for Ag^{+} and Fe^{3+}. The presence of Ag^{+} ions cause a blue shift (from yellow-green to green) and a decrease in the intensity of the P5DPB emission, while the addition of Fe^{3+} significantly quenches the P5DPB fluorescence. In addition, P5DPB satisfies the conditions for the construction of an energy transfer system with the commonly used Rhodamine B dye and shows great potential for the development of artificial light-harvesting systems. This work provides a new approach for the construction of energy transfer systems and a new reference for metal detection based on derivatized pillar[*n*]arenes, greatly enriching the applications of these systems.

Pillar[*n*]arenes [1–3] are important macrocyclic molecules formed by the cyclic arrangement of a certain number (*n*) of hydroquinone or 1,4-dimethoxybenzene units linked to each other by methylene bridges, generating rigid pillar-like π-electron-rich cavities with strong binding abilities to electron-poor species and having excellent potential for chemical modification [4,5]. Pillar[5]arene, with a cavity size around 5.5 Å that is sufficiently large to form sTable 1:1 complexes with small electron-poor molecules, have most widely been investigated to date [6–9]. Functionalization can endow pillar[*n*]arenes with new physical or chemical properties or generate completely new materials, leading to broader applications [10–14] and this area of investigation is rapidly growing. However, this functionalization may require quite tedious synthetic procedures. Functionalized pillar[*n*]arenes have initially been classified according to the degree of substitution, including monofunctionalized, difunctionalized, and perfunctionalized [15–19]. In addition to growing fundamental research, practical applications, which comprise chemosensors, organic light-emitting diodes, hydrogel materials, nanomaterials, *etc.*, are also increasing [20–26]. For example, Ma and his collaborators [27] synthesized a perfunctionalized pillar[5]arene based on 8-hydroxyquinoline, which introduced reactive sites for sensing metals and anions. A logic gate made up of Hg^{2+}, CN^{-} and this pillar[5]arene was then successfully fabricated. Moreover, functionalization also gave great impetus to improve the pillar[5]arene fluorescence performance. Gouda and co-workers [28] made full use of the BODIPY dye to synthesize a green-emissive pillar[5]arene. Due to the strong redshift of the emission wavelength after functionalization, this BODIPY-based pillar[5]arene meets the conditions of triggering the Forster resonance energy transfer (FRET) behavior with merocyanine. The strong research effort on functionalized pillar[5]arenes is continuing, revealing the great value of functionalized pillar[5]arenes as well as their impressive application potential.

In the present work, a new difunctionalized pillar[5]arene (P5DPB, Scheme 1), containing two 4,4′-(1,4-phenylenedi-2,1-ethenediyl) bis-pyridine (DPB) units on the pillar[5]arenes ring, was designed and synthesized (Schemes S1-S3 in Supporting information). DPB, as a typical dye, is a linear π-conjugated molecule that is often used in the research of artificial light-harvesting systems, metal-organic frameworks, light-emitting diodes, *etc.* [29]. Therefore, the introduction of DPB endows P5DPB with many new features. Compared with the ordinary pillar[5]arene [30,31], the intervention of a large hydrophobic conjugated group drastically changes the structure and induces a deformation of the columnar cavity, suppressing the basic aggregation-induced emission (AIE) property of the parent pillar[5]arene, and conversely introducing the new aggregation-caused quenching (ACQ) property [32,33]. Moreover, P5DPB serves as a metal coordination ligand [34–38]. Experiments show that the neutral pyridine of P5DPB specific recognition towards Ag^{+} and Fe^{3+}. The presence of Ag^{+} directly in-

* Corresponding author.
E-mail address: gyhxxiaoxin@163.com (X. Xiao).

https://doi.org/10.1016/j.cclet.2022.04.028
1001-8417/

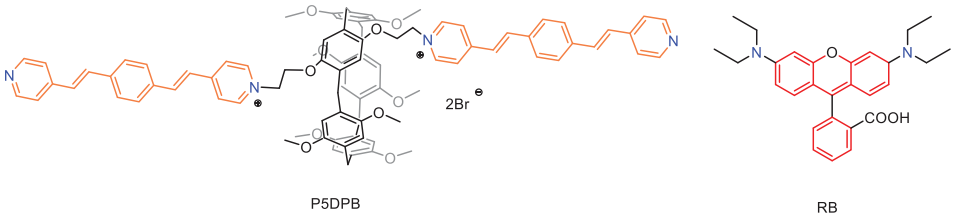

Scheme 1. The structures of P5DPB and RB.

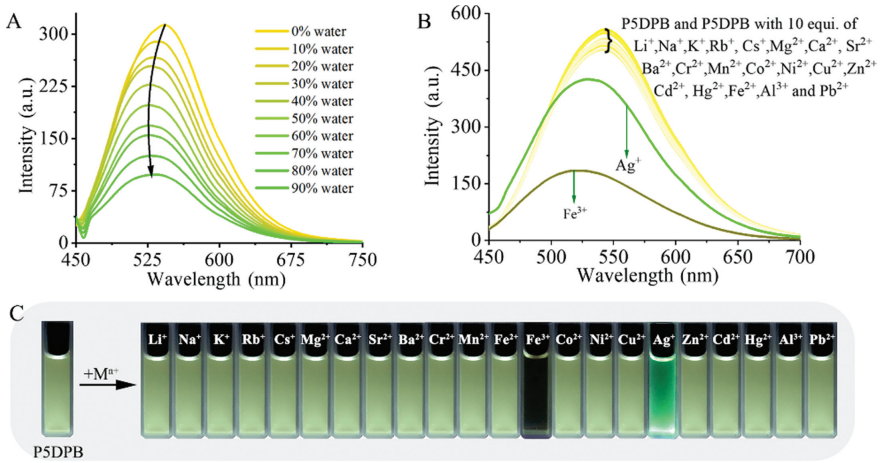

Fig. 1. Fluorescence spectra (λ_{ex} = 425 nm) of (A) P5DPB (20 μmol/L) in water/DMSO with increasing f_{water} and (B) P5DPB (20 μmol/L) in the presence of 10 equiv. of different metals in DMSO; (C) photographs of P5DPB solutions (20 μmol/L) in DMSO before and after the addition of different metals under UV irradiation.

duced the aggregation of P5DPB, further leading to a significant decrease in the emission intensity of P5DPB and a blue shift of wavelength from yellow to green, while the addition of Fe^{3+} quenches the P5DPB fluorescence. Finally, since the emission of P5DPB overlaps with the excitation of Rhodamine B (RB) dye to meet the necessary conditions for triggering the FRET system, P5DPB can construct a fast and simple FRET system with RB dye, indicating that it is a potential donor for an artificial light-harvest system [39–42]. The pillar[5]arene derivatives synthesized in this paper, which have the functions of metal detection and artificial light-harvest system, provide ideas for designing and synthesizing more and more practical pillar[5]arene derivatives, and promote pillar[5]arene derivatives to practical applications.

P5DPB is a pillar[5]arene derivative modified with two fluorescent conjugated DPB molecules and simultaneously possesses two hydrophilic pyridinium groups and two neutral pyridines that can easily coordinate with metals. Such a modification is of great significance to improve the P5DPB performance. For example, the emission wavelength of P5DPB is greatly red-shifted from the typical value of common pillar[5]arenes (about 325 nm) [30] to 542 nm by the modification with the large conjugate groups. The fluorescence characteristics are also changed. P5DPB no longer exhibits the typical aggregation-induced emission (AIE) effect of normal pillar[*n*]arenes. On the contrary, it exhibits the aggregation-caused quenching (ACQ) effect that most fluorescent compounds have (Fig. 1A). At a fixed 20 μmol/L concentration in a mixture of DMSO (good solvent) and water (poor solvent), the fluorescence intensity decreases from 313 a.u. to 97 a.u. (ΔI = 216 a.u.) as the water content is increased from 0 to 90%. What influenced the huge difference between P5DPB and the normal pillar[*n*]arenes was the introduction of large DPB molecules. The AIE effect of the normal pillar[*n*]arenes mainly originates from the aggregation of benzene rings to form rigid columnar structures of the cavity. However, due to the modification of the classical π-conjugated DPB molecules, the aggregation of P5DPB occurs mainly between DPB molecules, while the benzene rings of P5DPB are difficult to aggregate into rigid structures, so P5DPB mainly reflects the ACQ effect.

Meanwhile, the introduction of two neutral pyridines endows P5DPB with strong coordinating abilities and can thus be utilized in metal detection. The effect of the metal addition on the fluorescence response was probed for the alkali and alkaline-earth metals and several transition metals, using 10 equiv. of M^{n+}. As shown in Fig. 1B, Ag^+ and Fe^{3+} show the strongest change. The addition of Ag^+ reduces the P5DPB emission intensity and shifts the emission wavelength to blue, while the presence of Fe^{3+} significantly quenches the P5DPB emission, also with a blue shift. The effect of these metal additions is also visually evident under UV lamp irradiation. The emitted light of the solution changes to green in the presence of Ag^+ and is dramatically weakened by Fe^{3+} (Fig. 1C).

To further explore the interaction between the P5DPB and the above two metals, fluorescence titrations were carried out. As shown in Fig. 2B, the emission of P5DPB-Ag^+ decreases to about 288 a.u. and blueshifts by about 42 nm as the Ag^+ amount is increased. In addition to the visually evident light change from yellow to green (inset of Fig. 2B), the chromaticity coordinates also change dramatically from (0.35, 0.54) for P5DPB to (0.23, 0.36) for P5DPB-Ag^+, crossing the chromaticity diagram (Fig. S8 and Table S1 in Supporting information). The corresponding binding constant is calculated as 3.64×10^5 L/mol [34,37]. The detection limit of P5DPB towards Ag^+ is calculated as 2.45×10^{-6} mol/L (Fig. S9 in Supporting information) and other metal ions do not interfere with the Ag^+ detection process, except for the Fe^{3+} ion (Fig. S10 in Supporting information).

The reason for the fluorescence reduction and the Ag^+ detection mechanism was further studied. ^{1}H NMR titration experiments (Fig. 2A) show that the Ag^+ addition shifts the P5DPB H_a-H_g proton signals downfield, which is attributed to the deshielding effect of the Ag^+ coordination. More specifically, H_a shifts from 8.53 ppm to 8.72 ppm ($\Delta\delta$ 0.19 ppm), H_b, H_c, and H_g (overlapped in one observed peak) shift from 7.54 ppm to 8.01 ppm

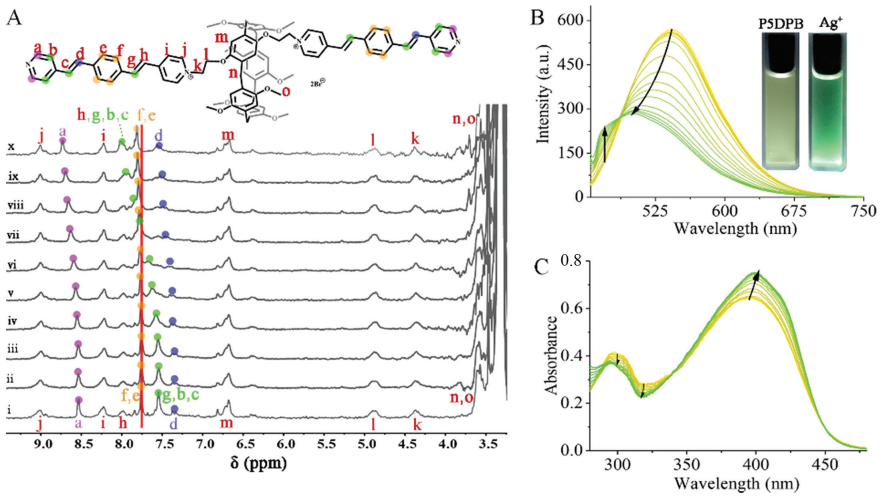

Fig. 2. (A) ^{1}H NMR titration of P5DPB (1 mmol/L in DMSO–d_6) with an increasing Ag^+ amount from 0 (i), 0.2 (ii), 0.7 (iii), 1.7 (iv), 2 (v), 4 (vi), 7 (vii), 10 (viii), 15 (ix) to 25 (x) equiv.; (B) fluorescence spectra of P5DPB (20 μmol/L in DMSO, λ_{ex} = 425 nm) with an increasing Ag^+ amount from 0 to 73 equiv.; (C) UV–vis spectra of P5DPB (20 μmol/L in DMSO) with an increasing Ag^+ amount from 0 to 3 equiv.

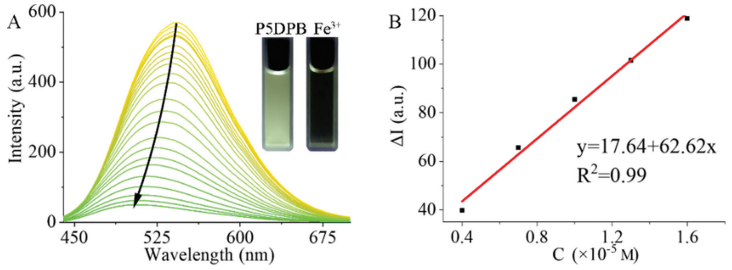

Fig. 3. The fluorescence spectra (A) of P5DPB (20 μmol/L) with the increasing amount of Fe^{3+} from 0 to 35 equiv. in DMSO at λ_{ex} = 425 nm, and the DL (B) plot of P5DPB detecting Fe^{3+}.

($\Delta\delta$ 0.47 ppm), H_d shifts from 7.34 to 7.56 ppm ($\Delta\delta$ 0.22 ppm) and H_f and H_e (also overlapped) shift from 7.75 to 7.81 ppm ($\Delta\delta$ 0.06 ppm). Meanwhile, the UV–vis absorption spectrum also changes as a result of the P5DPB-Ag^+ coordination interaction (Fig. 2C). The P5DPB absorbance at λ_{max} = 395 nm increases from 0.64 to 0.74 in the presence of Ag^+, which is mainly attributed to the n-π^* and π-π^* transition caused by the metal coordination. The intensity increases plateaus after the addition of 1 equiv. of Ag^+, indicating the formation of a 1:1 P5DPB-Ag^+ complex (Fig. S12 in Supporting information). Thus, the mechanism of detecting silver ions can be summarized as Ag^+ constructs a 1:1 stable assembly with P5DPB by coordination with the neutral pyridine, which facilitated the n-π^* and π-π^* transition between Ag^+ and P5DPB. The formation of the P5DPB-Ag^+ supramolecular polymers can be further demonstrated by scanning electron microscopy (SEM) and dynamic light scattering (DLS) analyses. The SEM images (Figs. S14 and S15 in Supporting information) show that the dispersed P5DPB molecules aggregate into regular, ordered morphologies due to the coordination interaction after the addition of Ag^+. Meanwhile, the DLS (Fig. S16 in Supporting information) shows an increase in the particle size from 6.71 nm to 136.5 nm in the presence of Ag^+, which also confirms the Ag^+-induced P5DPB aggregation.

P5DPB also has a good detection ability for Fe^{3+} with a low detection limit of 3.11×10^{-7} mol/L, $K_a = 2.63 \times 10^4$ L/mol [34,37] as well as a strong anti-interference ability (Fig. 4B and Fig. S10). The same methods described above for Ag^+ were used to further study the P5DPB-Fe^{3+}interaction. The NMR titration experiment (Fig. S17 in Supporting information) suggests that Fe^{3+} is also coordinated, like Ag^+, by the two neutral pyridines of P5DPB. However, the fluorescence titration reveals a different trend. As shown in

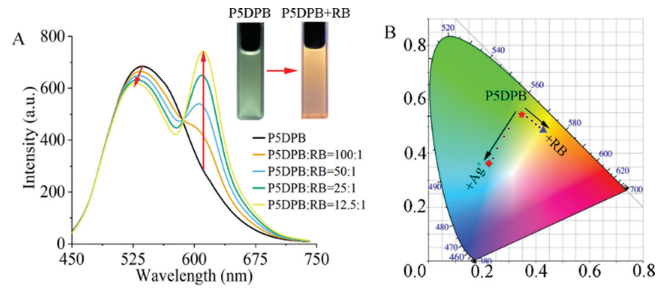

Fig. 4. (A) Fluorescence spectrum of P5DPB (20 μmol/L) with increasing amounts of RB and (insert) photographs of solutions before and after the addition of RB under UV irradiation at λ_{ex} = 365 nm; (B) chromaticity diagram with the coordinates of P5DPB (20 μmol/L, red star), P5DPB-RB (20 μmol/L, N_{P5DPB}/N_{RB} = 12.5:1, blue triangle) and P5DPB-Ag^+ (20 μmol/L, N_{P5DPB}/N_{Ag^+} = 1:40, red square).

Fig. 4A, as the concentration of Fe^{3+} increases, the P5DPB emission is rapidly quenched from 571 a.u. to 53 a.u., and a blue shift of about 40 nm can be also observed. In the corresponding UV–vis absorption study [38,43], since high concentrations of iron ions have a strong and broad absorption peak ranging from 200~550 nm, the P5DPB absorption gradually becomes more intense and broader as the Fe^{3+} concentration increases (Fig. S19 in Supporting information). It is worth emphasizing that the overlap region between the absorption of iron ions and the emission of P5DPB becomes larger with the increasing concentration of iron ions (Fig. S20 in Supporting information). Therefore, Fe^{3+} with strong UV absorption could easily absorb the excitation energy of the light source [38,41], and cause a significant decrease in the fluorescence of P5DPB. Fur-

thermore, experiments with NMR titration and binding constants showed that Fe^{3+}could likewise construct stable supramolecular assemblies *via* a neutral pyridine with P5DPB. Both DLS and SEM demonstrate the existence of this assembly, the P5DPB particle size (6.71 nm) increases to 197.11 nm in the presence of Fe^{3+}, while the SEM analysis shows an evolution from sparse and scattered objects to gathered and tight particles in the presence of Fe^{3+} (Figs. S14, S16 and S21 in Supporting information).

In addition to ion detection, P5DPB has another function. The major change observed in the P5DPB fluorescence emission can be exploited to construct a Forster resonance energy transfer (FRET) system. The P5DPB emission (542 nm) overlaps with the RB excitation (555 nm), which meets the basic condition of the energy transfer system (Fig. S22 in Supporting information). Therefore, P5DPB acts as the energy donor and RB as the energy acceptor. As shown in Fig. 4A, the addition of a small RB amount induces a gradual decrease ($\Delta I = 72$ a.u.) and blue shift ($\Delta\lambda = 9$ nm) of the P5DPB emission, while the RB emission at 580 nm is greatly increased (Fig. S23 in Supporting information), resulting in an emission light change from yellow-green to bright orange (inset of Figs. 4A and B). A solution of free RB at the same concentration does not show significant emission following excitation at 425 nm, which strongly certifies the construction of an energy transfer system between P5DPB and RB. The energy transfer efficiency from P5DPB to RB is estimated as 8.87% and the P5DPB quantum yield increases from 9.59% for free P5DPB to 19.1% in the presence of RB (Figs. S24 and S25 in Supporting information). These results indicate that P5DPB has great potential as an energy donor in the construction of artificial light-harvesting systems with Rhodamine B.

A new type of yellow-green luminescent pillar[5]arenes P5DPB was designed and synthesized by incorporating a classical fluorescent molecule (DPB). In comparison with common pillar[5]arenes, P5DPB exhibits many unique properties. For example, the neutral pyridine of P5DPB can be utilized for metal coordination and specific recognition of Ag^{+} and Fe^{3+}. The presence of Ag^{+} causes a significant blue shift (from yellow to green) and a decrease in emission intensity, while the addition of Fe^{3+} significantly quenches the P5DPB fluorescence. In addition, due to the dramatic redshift of the excitation wavelength caused by the chemical modification, P5DPB can be further used to construct an energy transfer system with Rhodamine B dye, with an estimated transfer efficiency of 8.87%. The work provides new ideas for the energy transfer system of pillar[*n*]arenes as donors and a new reference for metal detection, greatly enriching the applications of these systems.

Declaration of competing interest

There are no conflicts of interest.

Acknowledgments

This work was supported by the National Natural Science Foundation of China (No. 21861011) and the Innovation Program for High-level Talents of Guizhou Province (No. 2016–5657) and the Graduate Scientific Research Fund of Guizhou Province (No. YJSKYJJ[2021]021).

Supplementary materials

Supplementary material associated with this article can be found, in the online version, at doi:10.1016/j.cclet.2022.04.028.

References

[1] T. Ogoshi, S. Kanai, S. Fujinami, T. Yamagishi, Y. Nakamoto, J. Am. Chem. Soc. 130 (2008) 5022–5023.
[2] T. Ogoshi, T. Aoki, K. Kitajima, et al., J. Org. Chem. 76 (2011) 328–331.
[3] Y. Cai, Z. Zhang, Y. Ding, et al., Chin. Chem. Lett. 32 (2021) 1267–1279.
[4] Y. Ma, X. Chi, X. Yan, et al., Org. Lett. 14 (2012) 1532–1535.
[5] T. Ogoshi, J.I. Phenom, Macrocyclic Chem. 72 (2012) 247–262.
[6] N.L. Strutt, R.S. Forgan, J.M. Spruell, Y.Y. Botros, J. Stoddart, J. Am. Chem. Soc. 133 (2011) 5668–5671.
[7] K. Kitajima, T. Ogoshi, T. Yamagishi, Chem. Commun. 50 (2014) 2925–2927.
[8] L. Escobar, P. Ballester, Chem. Rev. 121 (2021) 2445–2514.
[9] B.L. Ho, D. Tian, J. Liu, et al., Inorg. Chem. 55 (2016) 10580–10586.
[10] H. Behera, L. Yang, J.L. Hou, Chin. J. Chem. 38 (2020) 215–217.
[11] X. Yuan, Y. Cai, L. Chen, et al., Separ. Purif. Technol. 230 (2020) 115843.
[12] T. Kakuta, T. Yamagishi, T. Ogoshi, Acc. Chem. Res. 51 (2018) 1656–1666.
[13] Y. Cai, X. Yan, S. Wang, et al., Inorg. Chem. 60 (2021) 2883–2887.
[14] C. Peng, W. Liang, J. Ji, et al., Chin. Chem. Lett. 32 (2021) 345–348.
[15] N.L. Strutt, H. Zhang, S.T. Schneebeli, J.F. Stoddart, Acc. Chem. Res. 47 (2014) 2631–2642.
[16] X. Xu, V.V. Jerca, R. Hoogenboom, Angew. Chem. Int. Ed. 59 (2020) 6314–6316.
[17] D. Strilets, S. Fa, A. Hardiagon, et al., Angew. Chem. Int. Ed. 132 (2020) 23413–23419.
[18] M. Cheng, G. Li, W. Xu, et al., Dyes Pigment. 194 (2021) 109646.
[19] Y. Cai, S.A. Ansari, K. Fu, et al., J. Hazard. Mater. 405 (2021) 124214.
[20] B. Liu, X. Lu, X. Liao, et al., Appl. Surface Sci. 566 (2021) 150739.
[21] J. Sun, Y. Dai, Y. Hou, et al., J. Phy. Chem. A 125 (2021) 2344–2355.
[22] S. Yu, Y. Wang, S. Chatterjee, et al., Chin. Chem. Lett. 32 (2021) 179–183.
[23] L. Chen, Y. Wang, Y. Wan, et al., Chem. Eng. J. 387 (2020) 124087.
[24] H. Zhang, J. Han, C. Li, Polym. Chem. 12 (2021) 2808–2824.
[25] K. Zhong, S. Lu, W. Guo, et al., J. Mater. Chem. A 9 (2021) 10180–10185.
[26] G.T. Williams, C.J.E. Haynes, M. Fares, et al., Chem. Soc. Rev. 50 (2021) 2737–2763.
[27] X.Q. Ma, Y. Wang, T.B. Wei, et al., Dyes Pigment. 164 (2019) 279–286.
[28] C. Gouda, D. Barik, C. Maitra, et al., J. Mater. Chem. C 9 (2021) 2321–2333.
[29] X.L. Ni, S. Chen, Y. Yang, Z. Tao, J. Am. Chem. Soc. 138 (2016) 6177–6183.
[30] J.F. Chen, G. Meng, Q. Zhu, S. Zhang, P. Chen, J. Mater. Chem. C 7 (2019) 11747–11751.
[31] X. Zhu, J. Zhao, F. Dai, et al., Spectrochim. Acta Part A: Mol. Biomol. Spectrosco. 250 (2021) 119381.
[32] R. Hu, N.L.C. Leung, B.Z. Tang, Chem. Soc. Rev. 43 (2014) 4494–4562.
[33] Y. Hong, J.W.Y. Lama, B.Z. Tang, Chem. Soc. Rev. 40 (2011) 5361–5388.
[34] Y. Yang, X.L. Ni, T. Sun, H. Cong, G. Wei, RSC Adv. 4 (2014) 47000–47004.
[35] G. Zhou, X. Zhang, X.L. Ni, J. Hazard. Mater. 384 (2020) 121474.
[36] G. Heo, R. Manivannan, H. Kim, et al., Sens. Actuators B: Chem. 297 (2019) 126723.
[37] M. Zhu, M. Yuan, X. Liu, et al., Org. Lett. 10 (2008) 1481–1484.
[38] R.M. Wen, S.D. Han, G.J. Ren, et al., Dalton Trans. 44 (2015) 10914–10917.
[39] X.L. Lia, Y. Wang, M.H. Zhang, et al., Dyes Pigment. 197 (2022) 109895.
[40] X.M. Chen, Q. Cao, H.K. Bisoyi, et al., Angew. Chem. Int. Ed. 59 (2020) 10493–10497.
[41] G. Sun, M. Zuo, W. Qian, et al., Green Synth. Catal. 2 (2021) 32–37.
[42] M. Rao, W. Wu, C. Yang, Green Synth. Catal. 2 (2021) 131–144.
[43] B.L. Ho, D. Tian, J. Liu, et al., Inorg. Chem. 55 (2016) 10580–10586.